PROCEEDINGS OF SPIE

Femtosecond laser inscribed advanced calibration phantom for optical coherence tomography (OCT)

Lu, Yang, Gordon, Neil, Coldrick, Benjamin, Ibrahim, Izzati, Mezentsev, Vladimir, et al.

Femtosecond laser inscribed advanced calibration phantom for optical coherence tomography (OCT)

Yang Lu*[a], Neil Gordon[a], Benjamin Coldrick[b], Izzati Ibrahim[b], Vladimir Mezentsev[a], David Robinson[c], Kate Sugden[a]

[a]Aston Institute of Photonic Technologies, Aston University, Birmingham, B4 7ET, UK;
[b]Optimec Limited, Unit B3, The Haysfield, Spring Lane North, Malvern, WR14 1GF, UK;
[c]Arden Photonics Ltd., Royston House, 267 Cranmore Boulevard, Solihull, B90 4QT, UK;

ABSTRACT

Optical coherence tomography (OCT) has developed rapidly and is widely used in different fields such as biomedicine and optometry. The characterization and calibration of OCT systems is essential when testing the system and during normal use to ensure that there is no misalignment or distortion that could affect clinical decisions. Imaging distortion is a significant challenge for OCT systems when viewing through non-planar surfaces. Here we present a new multi-purpose plano-convex OCT phantom which is designed to be used for OCT characterization and calibration as well as to validate the post-processing algorithm for the imaging distortion of the OCT systems. A femtosecond laser direct writing technique is used to fabricate this phantom which consists of a landmark layer with radial lines at a 45-degree angular spacing inscribed at 50μm in apparent depth (AD) underneath the planar surface. Below that there are a further 8 layers of a spherical inscription pattern which has a 150μm (in AD) separation between each layer. The first spherical layer is located at 150μm (in AD) underneath the planar surface. Due to the laser power loss when travelling through the deeper layer, an increased power is applied to the deeper layers. The spherical pattern overcomes orientation issues seen with existing calibration phantoms. The landmark layer is applied so that it can easily tell the exact location when scanning which will also benefit the image distortion correction process.

Keywords: optical coherence tomography (OCT), femtosecond laser inscription, OCT phantom, femtosecond laser direct writing, OCT calibration phantom, OCT image distortion, OCT phantom fabrication

1. INTRODUCTION

Optical coherence tomography (OCT) is an imaging technique which can provide a cross-sectional non-invasive real-time in-vivo image by using low-coherence interferometry [1]. OCT has been widely used in the field such as biomedicine and medicine (i.e. ophthalmology) since it was firstly demonstrated by Huang et al. in 1991 [1]. Since then, OCT systems have developed into different types including TD-OCT in 1991 [1], and FD-OCT which has two subsets (SS-OCT and SD-OCT) [2] and a growing number of companies have commercialized OCT systems [2]. However, to date, there is no standard approach to be applied in order to calibrate and measure the performance across different systems quantitatively during the installation process and day to day operation. Therefore, a universal multi-purpose phantom which can act as an optical ruler is needed to meet this requirement.

Previously, different methods have been presented to fabricate phantoms such as tissue-mimicking [3] and retinal phantom [4]. However, those methods do not address to all the requirements to quantitatively calibrate and assess the OCT system and associated image distortion when imaging through a curved surface. Femtosecond laser direct writing technique has been used previously for the purpose of phantom inscription at Aston [5], where a non-planar multi-purpose phantom was developed [6] where the planar side could be used for a standard assessment and calibration while the curved side could be used to test the validity of the post-processing algorithm for the image distortion. However, this phantom was inscribed with grid pattern that requires a higher degree of alignment in terms of the angle of the sample to generate a useful calibration phantom for the OCT operator.

*Email: luy12@aston.ac.uk; Phone: +44 121 204 3616

Here, a new plano-convex OCT phantom is presented to simplify the alignment issues and that includes a landmark layer that can be used to orientate the sample. The phantom can fulfil the purpose of a standard calibration phantom but can also be used to detect distortion and ultimately correct for system distortion through the appropriate use of software algorithms or test the effectiveness of existing algorithms.

2. EXPERIMENTAL SETUP

A mode-locked ytterbium-doped femtosecond laser system (Amplitude s-Pulse HP) generated laser pulse which has a central wavelength of ~1026 nm and a repetition rate range of 1-100kHz. The laser power can be varied from 0% to 100% of the total power with the use of an attenuator. The phantom was inscribed at 100kHz and the laser power was set to be varied from 40% to 100% (the average power was 117mW for 40% and 311mW for 100%). A power meter is positioned below the inscription lens to monitor the output power. This objective lens is from the Mititoyo MPlan Apo NIR series which has a magnification of 100x and a numerical aperture of 0.5 which results of a spot size of ~2μm. The laser system is equipped with a high accuracy and high-resolution XY air-bearing stage and a separate mechanical Z-axis with a goniometer mounted on a granite base with which can be software controlled through an Aerotech (A3200) automation controller. The phantom is inscribed on a plano-convex lens (LA4380, Thorlabs) made of fused silica with a refractive index of 1.461. The schematic diagram of the femtosecond laser system set up is shown in Figure 1. The femtosecond laser direct writing technique leads to a permanent refractive index change due to the non-linear multi-photon absorption. The phantom is inscribed through the planar side to minimize aberration effects.
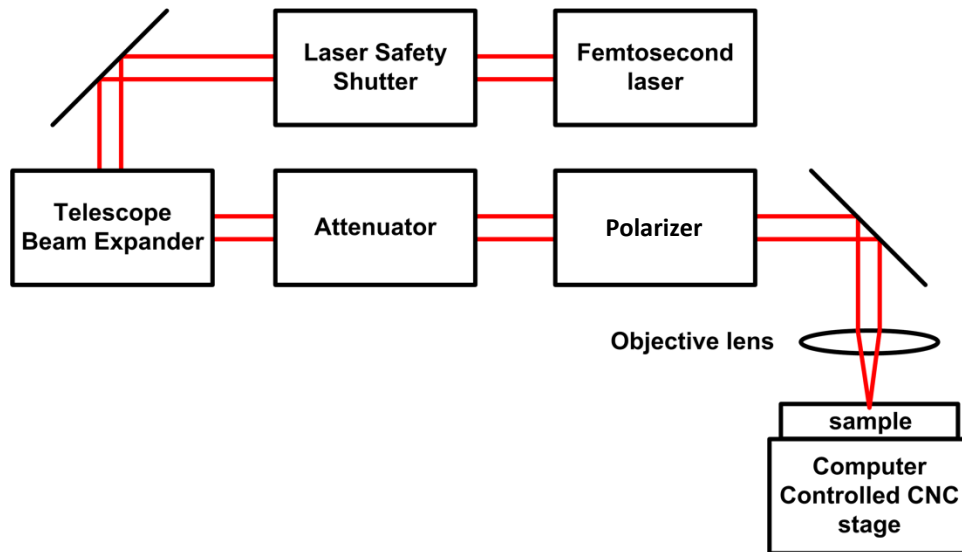

Figure 1. Schematic diagram of the femtosecond laser system setup. The laser has a central wavelength of 1026nm, the repetition rate can be varied from 1kHz to 100kHz, the output laser power can be varied from 0% to 100% and the objective lens is 100x.

The phantom was characterized using an optical microscope (Axioskop 2 MOT Plus, Zeiss) and an OCT system (Optimec is830 SD-OCT system). For the microscope measurement, both the 5x and the 20x objective lens were used to characterize the phantom, where the 5x objective lens was used to capture a top-view pattern image and the 20x objective lens was used to investigate the layer separation and the linewidth data of the phantom. The Optimec is830 SD-OCT system was used for the OCT characterization. This system is equipped with a super luminescent diode (SLD) light source and a fiber coupler acting as a beam splitter divides the light between the sample and the reference arm [7]. A spectrometer was used to analyze the return reflection combined between the reference arm and the sample scanned by a micro-electrical mechanical (MEMs) mirror system [7]. This OCT system has a central wavelength of 830nm, an axial resolution of 12μm (in air), a lateral resolution of 30μm and a sensitivity of 107dB at 1.2kHz, which has a measurement volume of 20mm x 20mm x 6 mm [7].

3. PHANTOM DESIGN AND FABRICATION

The phantom pattern shown in Figure 2 consists of one landmark layer located at 50μm (in apparent depth (AD)) below the surface and 8 layers of the test pattern where the first layer is located at 150μm (in AD) below the surface and each layer has a separation of 150μm so that in total the inscribed depth reaches to 1200μm (in AD, so that the real depth (RD) is 1753.2μm (1200μm x 1.461 (the refractive index of fused silica) = 1753.2μm). A set of radial lines is inscribed in the landmark layer that have an angular separation of 45 degrees. This design enables the end user to easily control the location of the phantom relative to the field of view of the OCT system. With the previous grid pattern, the orientation presented a problem since it affected the separation of the points. To overcome this difficulty, a spherical pattern is inscribed on each layer in this phantom design. Each layer includes a set of 40 circles with increasing radius (i.e. a radius difference of 254μm), where the radius range varies from 0.254mm to 10.16mm. Due to the power loss when penetrating to deeper layers, each layer is inscribed with different laser powers between 40% and 100% of the total laser output power, where 40% of the laser power was used to inscribe the top layer and 100% of the laser power was used to inscribe the deepest layer. The laser power difference for each layer is identical, with the aim of obtaining a consistent linewidth for each layer. The pattern was inscribed on a planar-convex fused silica lens which has a central thickness of 3.8mm and an edge thickness of 2mm. The moving speed for the stage was set to 4mm/s and the writing speed was set to 1mm/s.

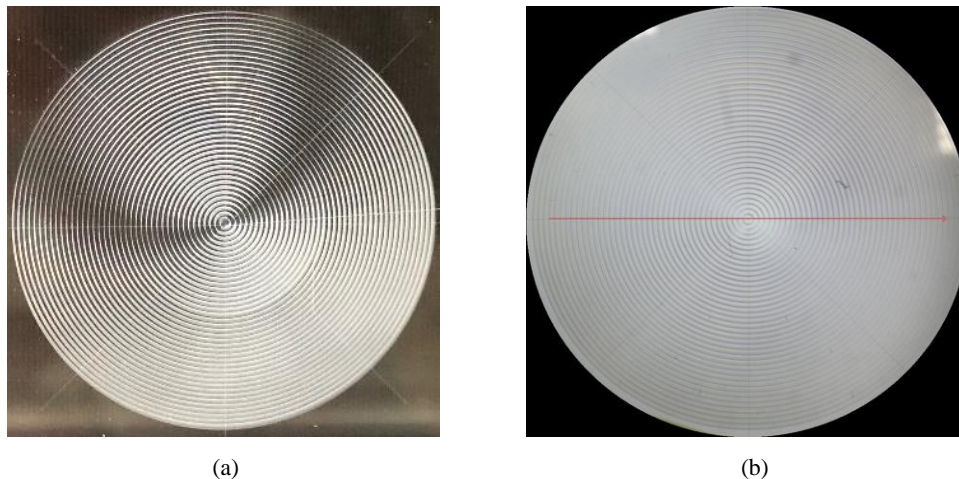(a)   (b)

Figure 2. Phantom design pattern: (a) the pattern initially tested and fabricated on a planar substrate; (b) the pattern fabricated on a curved lens (LA4380, Thorlabs) viewing under an OCT system (Optimec is830 SD-OCT system).

Alignment is always a challenge when placing a sample on the CNC stage to ensure its flatness, especially for a non-planar substrate which increases the difficulty. Four equidistant points on the edge were chosen to assist the alignment. A CCD camera was used in this alignment process to determine the focus position along with the adjustment through both software control of the CNC stage and the manual adjustment of a goniometer base. To ensure a high degree of alignment of the sample, a software program was designed to inscribe various minor marks to verify the surface and the alignment. The alignment is adjusted until at least three points on the edge were focused at the same position, at which point the alignment process is completed and the fourth point can be used to verify the alignment. The program was set to start at the center of the surface. The laser inscription was started from the lowest layer (i.e. the deepest layer) to avoid scattering caused by modified regions.

4. RESULTS AND DISCUSSIONS

Both an optical microscope (Axioscope 2 MOT Plus, Zeiss) and an OCT system (Optimec is830) were used to characterize the OCT phantom. The microscope measurement provided information on the linewidth of the inscription in the XY plane which is parallel to the translation stage, and the layer depth for the Z-axis while the OCT system provided a cross-sectional image or a depth profile of the phantom. The comparisons between the setting parameters and the measured parameters of the layer depth are presented in Figure 3 to show the accuracy of the laser fabrication. It can be seen that there is a high

degree of alignment accuracy so that the measured values are almost identical to the designed value (with +/− 2µm error tolerance) (i.e. the landmark layer was set to 50µm below the planar surface and the measured value of the landmark layer depth was 50.945µm).
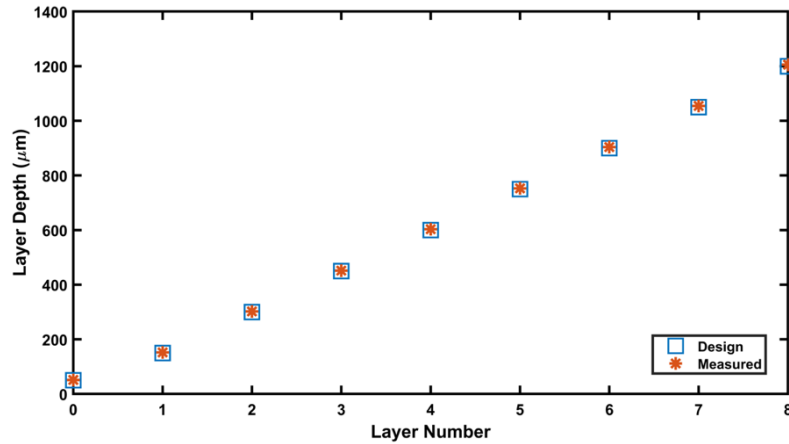

Figure 3. The comparison of design parameter values and measured values from the microscope measurement of the OCT phantom by using a 20x objective lens. The layer depth is in apparent (measured) depth (AD).

The microscope images taken using a 5x objective lens are shown in Figure 4(a) and (b) which Figure 4(a) was taken from a planar surface and Figure 4(b) was taken from a curved surface of the phantom. Figure 4(a) shows that there is high degree of agreement between the design value (i.e. 254µm between each circle) and the measured value for the spherical radius (i.e. ~254 ± 1um between each circle). Figure 4(b) shows a microscope image when viewing the phantom from a curved surface. It can be seen that the radius difference between each circle is ~258µm ± 1um, which has a 4µm difference to the measurement taken from the planar surface. It may be due to the curvature of the lens that distorted the image slightly, however, the spherical separation remains as ~258µm ± 1um for each circle that can indicate that the sample is not misaligned. Figure 4 (c) and (d) show the linewidth in the XY plane via an optical microscope was measured. The microscope image was acquired using a 20x objective lens taken from the planar side at the 5th layer (at 752.485µm in AD below the planar surface) showing a linewidth of 6.3µm. In Figure 4(d), the microscope image was captured by using a 20x objective lens taken from the planar side at the 7th layer (at 1054.252µm in AD below the planar surface) showing a linewidth of 6.3µm. Therefore, by varying the laser power, the linewidth of the inscription can be consistent for each layer.

(a)

(b)

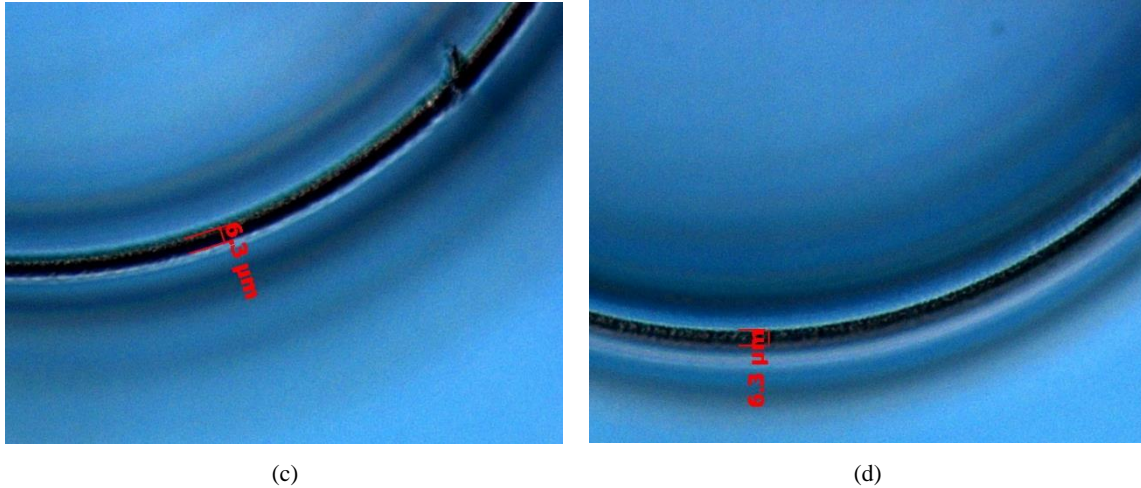<center>(c)   (d)</center>
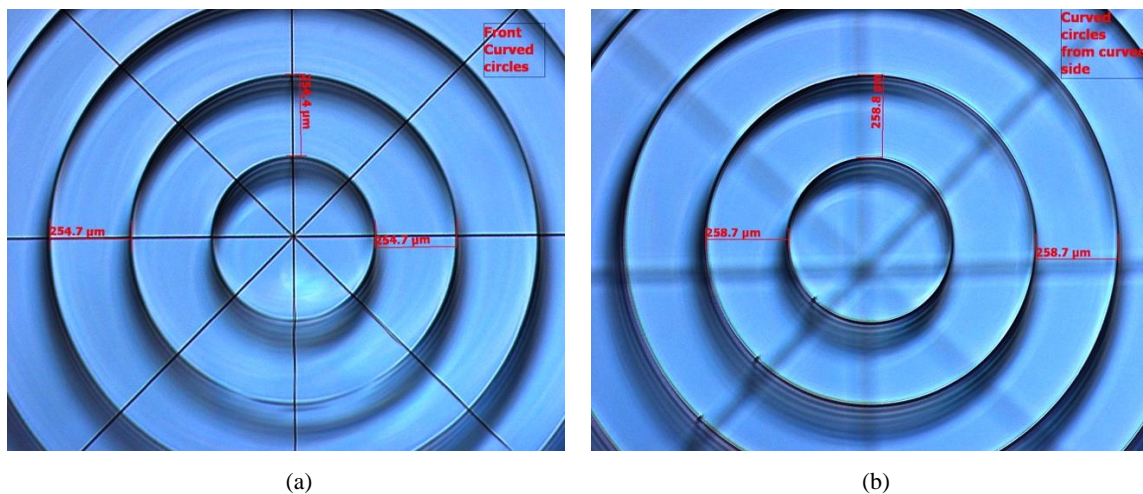
Figure 4. (a) Microscope image using a 5x objective lens taken from the planar side of the phantom; (b) microscope image using a 5x objective lens taken from the curved side of the phantom; (c) microscope image using a 20x objective lens taken from the planar side at the 5th layer (at 752.485μm in AD below the planar surface) showing a linewidth of 6.3μm; (d) microscope image using a 20x objective lens taken from the planar side at the 7th layer (at 1054.252μm in AD below the planar surface) showing a linewidth of 6.3μm.

Subsequent to the microscope characterization, the OCT phantom was then characterized using an OCT system (Optimec is830 system). Example images taken by this system are shown in Figure 5 and Figure 6 that verify the phantom design and illustrate its potential use as a calibration phantom. A solid line for the landmark layer (shown in yellow) indicates that the scan position went through the central point and parallel to a landmark line, this is helpful if using this phantom to correct the image distortion since it gives a known cross-sectional position. Figure 5 shows the view from the planar side of the phantom which is a non-distorted image. It be seen that the landmark layer and all eight layers of the pattern are clearly visible in the OCT image. The parameter measurement on the OCT image matches the designed parameters and the microscope measurements.
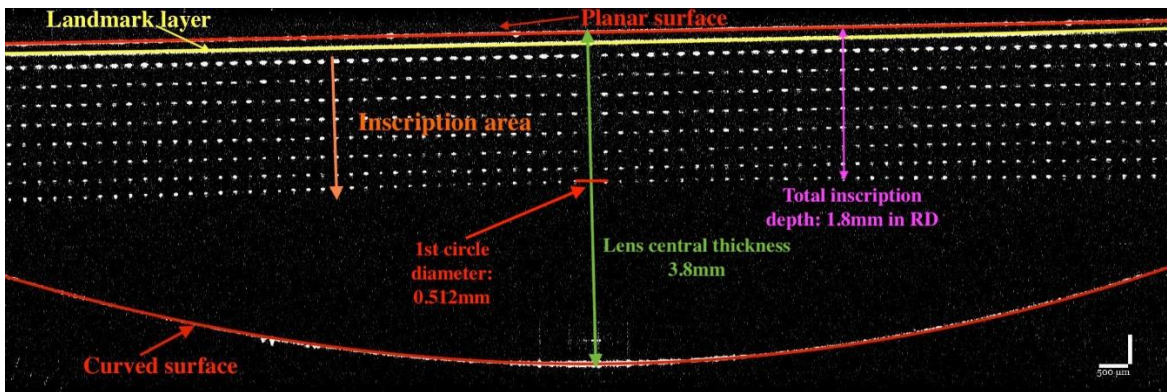

Figure 5. OCT image taken from the planar surface of the phantom. The scan pattern FOV is 19.00mm x 5.42mm. The scale bar is 500μm. The value indicated on this image is in real depth as the refractive index is applied.

Figure 6 shows an image was taking from the curved surface of the OCT system. The pattern is distorted because of the curvature of the lens. For example, an ophthalmic application measuring a patient's eye, the OCT system would use a post-processing algorithm to correct the distortion but this assumes a given curvature and refractive index of the lens. Moreover, the central area of this OCT image is much weaker compared with the image taken from the planar surface and the spot seems to be expanded vertically.
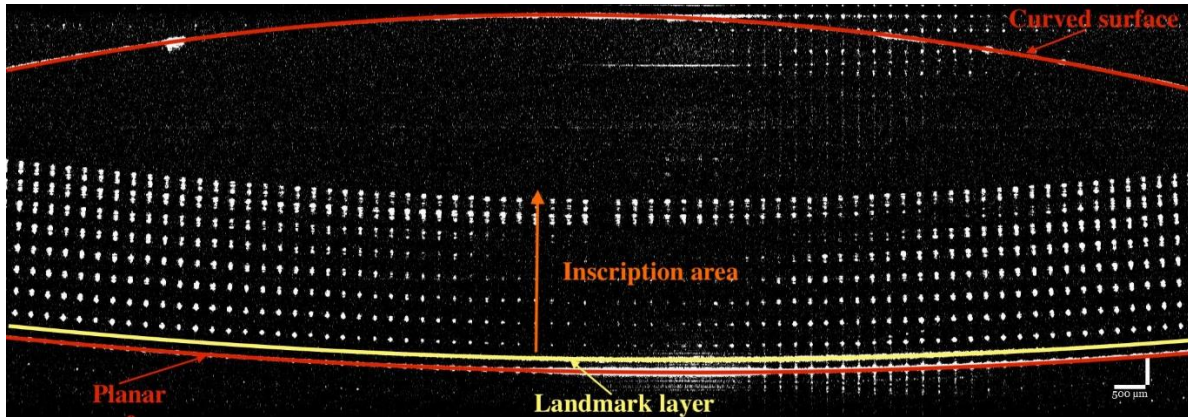
Figure 6. OCT image taken from the curved surface of the phantom. The scan pattern FOV size is 19.00mm x 5.42mm. The scale bar is 500μm.

5. CONCLUSIONS

In summary, for the first time, a spherical pattern with a landmark layer is used in a new phantom design. This phantom can be used to assess, characterize and calibrate the OCT system that are designed to measure non-planar samples. The spherical pattern overcome issues previously observed that were caused by the unknown alignment angle when measuring the phantom with the OCT system. With this new phantom design, the post-processing image distortion correction can be validated since the landmark layer can confirm the exact location and orientation. The planar side can then provide a standard reference when comparing to the curved side. This phantom can be effectively applied to detect and potentially quantitatively correct the distortion based on a self-comparison method. By using the planar side as a standard reference (i.e. non-distorted image) and comparing it with the distorted image, any post-processing algorithms can be validated to ensure optimum system performance.

ACKNOWLEDGEMENTS

REFERENCES

[1] Huang, D., Swanson, E. A., Lin, C. P., Schuman, J. S., Stinson, W. G., Chang, W., Hee, M. R., Flotte, T., Gregory, K., Puliafito, C. A. and Fujimoto, J. G., "Optical coherence tomography," Science 254(5035), 1178-1181 (1991).
[2] Fujimoto, J., and Swanson, E., "The Development, Commercialization, and Impact of Optical Coherence Tomography," Investigative ophthalmology & visual science vol. 57, 9 (2016).
[3] Kennedy, B. F., Loitsch, S., McLaughlin, R. A., Scolaro, L., Rigby, P., and Sampson, D. D., "Fibrin phantom for use in optical coherence tomography," Journal of biomedical optics, 15(3) (2010).
[4] Baxi J., Calhoun, W.R., Sepah, Y.J., Hammer, D.X., Ilev, I., Pfefer, T.J., Nguyen, Q.D., Agrawal, A., "Retina-simulating phantom for optical coherence tomography," Journal of biomedical optics, Sep;19(2) (2013).
[5] Lee, G. C., Rasakanthan, J., Woolliams, P. D., and Sugden, K., "Fabrication of high quality optical coherence tomography (OCT) calibration artefacts using femtosecond inscription," Biophotonics: Photonic Solutions for Better Health Care III , Vol. 8427, International Society for Optics and Photonics (2012).
[6] Lu, Y., Gordon, N., Robinson, D., Coldrick, B., Mezentsev, V., Menduni, F., Fratini, A. and Sugden, K., "Non-planar calibration phantoms for optical coherence tomography," Advanced Fabrication Technologies for Micro/Nano Optics and Photonics XI, Vol. 10544, International Society for Optics and Photonics (2018).
[7] Coldrick, B. J., Richards, C., Sugden, K., Wolffsohn, J. S., and Drew, T. E., "Developments in contact lens measurement: A comparative study of industry standard geometric inspection and optical coherence tomography," Contact Lens and Anterior Eye 39(4), 270-276 (2016).